# Unique-region phosphorylation targets LynA for rapid degradation, tuning its expression and signaling in myeloid cells

Ben F. Brian IV[1], Myra G. Nunez[1], Kathryn L. Schwertfeger[1,2,3], Tanya S. Freedman[1,2,4,*]

[1]Department of Pharmacology, University of Minnesota, Minneapolis, MN 55455, USA.

[2]Center for Immunology and Masonic Cancer Center, University of Minnesota, Minneapolis, MN 55455, USA.

[3]Department of Laboratory Medicine and Pathology, University of Minnesota, Minneapolis, MN 55455, USA.

[4]Center for Autoimmune Diseases Research, University of Minnesota, Minneapolis, MN 55455, USA.

[*]To whom correspondence should be addressed: tfreedma@umn.edu

## Abstract

The activity of Src-family kinases (SFKs), which phosphorylate immunoreceptor tyrosine-based activation motifs (ITAMs), is critical factor regulating myeloid-cell activation. In a previous paper (Freedman *et al.*, 2015) we showed in macrophages that the SFK LynA is uniquely susceptible to rapid ubiquitin-mediated degradation, functioning as a rheostat regulating ITAM signaling. We now report the mechanism by which LynA is preferentially targeted for degradation and how cell specificity is built into the LynA rheostat. Using genetic and biochemical analysis, we found that the E3 ubiquitin ligase c-Cbl preferentially targets LynA via tyrosine 32 in its unique insert region. This orthogonal mode of c-Cbl recognition depresses the steady-state level of macrophage LynA. Mast cells, however, express little c-Cbl and have correspondingly high steady-state levels of LynA. Upon activation, mast-cell LynA is not rapidly degraded, and SFK-mediated signaling is amplified relative to macrophages. Cell-specific c-Cbl expression therefore builds cell specificity into the LynA checkpoint.

## Introduction

Phosphorylation of immunoreceptor tyrosine-based activation motifs (ITAMs) by Src-family kinases (SFKs) is the first step in the activation of an innate immune response during a pathogen encounter. Initiation of cell-activating signaling typically occurs within clusters of ITAM-coupled receptors such as

27 FcγR (1) or the hemi-ITAM Dectin-1 (2, 3), nucleated by highly multivalent binding to immunoglobulin-
28 G-decorated pathogens or fungal cell-wall β-glucans respectively. Together, SFKs and phosphorylated
29 ITAMs trigger activation of the tyrosine kinase Syk (4). The SFKs and Syk then drive activation of
30 membrane-proximal signaling through adaptor proteins, cytoskeleton-modulating proteins such as the
31 FAK/Pyk2 kinases and Paxillin, and Tec kinases, which activate second-messenger pathways via
32 phosphoinositide 3-kinase and phosphoinositide phospholipases Cγ (PI3K and PLCγ1/2 respectively).
33 Ultimately, these early events lead to downstream signaling through Erk1/2 and other pathways (4). As
34 the byproducts of activated macrophages can be toxic (*e.g.* release of reactive oxygen species) and
35 drive inflammation (*e.g.* release of tumor necrosis factor α), the responsiveness of innate immune cells
36 must be tightly regulated (5-8).

37 Multiple mechanisms work together to tune the responsiveness of macrophages and other myeloid
38 cells, including negative regulation by the phosphatases CD45 and CD148 (5, 9, 10), cytoskeletal
39 barriers to diffusion (11), signaling via immunoreceptor tyrosine inhibitory motifs (ITIMs) (12) and
40 inhibitory ITAMs (13, 14), and degradation and mislocalization of signaling molecules targeted for
41 polyubiquitination by ubiquitin ligases (15, 16). The SFKs, which in myeloid cells typically include Fgr,
42 Fyn, and two splice forms each of Hck and Lyn, may also have positive and negative functions (12, 17-
43 19). Layered onto the traditional positive- and negative-regulatory roles of the SFKs, we have shown
44 that activated LynA (the longer of the two Lyn splice forms) is rapidly and specifically targeted for
45 polyubiquitination and degradation, forming the basis of a signaling checkpoint that blocks spurious
46 macrophage activation (20). The mechanism preferentially targeting LynA for polyubiquitination and the
47 molecular basis of this selectivity have not been elucidated previously.

48 Unlike Dectin-1 and FcγR signaling in macrophages, which is typically triggered in the context of
49 pathogen-induced μm-scale clusters of receptors (5, 9, 20), mast-cell FcεR signaling has a low
50 threshold for activation-- small or even monovalent antigen-IgE complexes are sufficient to induce a
51 signaling response (21, 22). Like macrophages, mast cells express LynA, and this disparity in receptor
52 sensitivity has not previously been explained.

53 This paper describes the mechanism by which active LynA is selectively recognized and rapidly
54 degraded, tuning its activation kinetics and its steady-state protein levels in a cell-specific manner. To
55 reveal the requirements for LynA degradation, we synchronized receptor-independent SFK activation
56 using the designer inhibitor 3-IB-PP1 (23-25), which specifically inhibits a variant of the SFK-inhibitory
57 kinase Csk ($Csk^{AS}$) (20, 25, 26). Csk is responsible for phosphorylating a key inhibitory tyrosine in the
58 C-terminus of all the SFKs. Inhibiting $Csk^{AS}$ leads to rapid and robust SFK activation due to the loss of
59 the dynamic equilibrium between Csk and the phosphatases CD45 and CD148 (27, 28). We showed
60 previously that SFK activation induced via 3-IB-PP1 treatment leads to the phosphorylation of the E3
61 ubiquitin ligase c-Cbl and the preferential polyubiquitination and degradation of the SFK LynA, but it
62 was not clear whether these two events were linked. Using knockdown, overexpression, and genetic
63 models, we now demonstrate that c-Cbl, but not its homolog Cbl-b, controls the steady-state expression
64 of LynA and mediates its rapid degradation upon activation in macrophages. LynA is targeted by c-Cbl
65 via a phosphorylation site, Tyr32 within its unique region, a mode of interaction distinct from the slower-
66 phase action of c-Cbl and other E3 ligases on LynB and the other SFKs. Finally, we have discovered
67 that the LynA checkpoint is cell specific. In mast cells, which express very little c-Cbl but abundant Cbl-
68 b, LynA is not rapidly degraded upon activation, helping to explain why mast cells have a lower
69 activation threshold than macrophages.

## 70 Results

### 71 c-Cbl mediates steady-state and activation-induced degradation of LynA in macrophages

72 We reported previously that activated LynA is rapidly polyubiquitinated and degraded in $Csk^{AS}$
73 macrophages treated with the $Csk^{AS}$ inhibitor (SFK activator) 3-IB-PP1 (20). To identify the responsible
74 E3 ubiquitin ligase, we tested the effects of knocking down the expression of candidate ligases using
75 small interfering (si)RNA. $Csk^{AS}$ bone-marrow-derived macrophages (BMDMs) were transfected with
76 non-targeting control RNA or with siRNA constructs targeting c-Cbl or Cbl-b, known modulators of ITAM
77 signaling in both adaptive and innate immune cells (12, 15, 29). Resting $Csk^{AS}$ BMDMs were treated

78 with 3-IB-PP1 for up to 5 min to activate the SFKs and initiate bulk degradation of LynA. Immunoblots
79 of whole-cell lysates showed efficient and specific knockdown **(Figure 1A)** of c-Cbl protein (70%
80 reduced) and Cbl-b protein (60% reduced) **(Figure 1B)**.

81 Knockdown of c-Cbl led to a delay in the degradation of activated LynA, with 1 min 3-IB-PP1 treatment
82 reducing LynA by 30% in c-Cbl knockdown BMDMs compared to 61% and 64% in Cbl-b knockdown
83 and control BMDMs, respectively **(Figure 1C)**. c-Cbl knockdown also increased the level of steady-
84 state LynA by 60% **(Figure 1D)**. The impaired degradation and increased steady-state LynA expression
85 together resulted in pronounced elevations in LynA protein in the first minutes of 3-IB-PP1 treatment;
86 after 1 min of 3-IB-PP1 treatment, LynA was elevated 2.9-fold in cCbl-deficient BMDMs relative to
87 control. Although it has been shown previously that c-Cbl and Cbl-b can have redundant functions (30,
88 31), we were unable to detect any role for Cbl-b in the steady-state or activation-induced degradation of
89 LynA.

90 To test whether the residual LynA degradation was due to incomplete knockdown, we also generated
91 *Csk$^{AS}$Cbl$^{-/-}$* mice to test LynA degradation in BMDMs lacking any c-Cbl expression. As with siRNA
92 knockdown, total c-Cbl knockout impaired LynA degradation in BMDMs **(Figure 1E)**; Cbl-b expression
93 in Csk$^{AS}$c-Cbl$^{-/-}$ BMDMs remained comparable to wild-type levels **(Figure 1F)**. Complete loss of c-Cbl
94 caused a more profound impairment of LynA degradation during the first few minutes of 3-IB-PP1
95 treatment **(Figure 1G)** a dramatic increase in steady-state LynA protein (up to 6-fold higher than in c-
96 Cbl$^{+/+}$ cells, **Figure 1H**). As in the knockdown experiments, LynA degradation in c-Cbl$^{-/-}$ BMDMs was not
97 fully eliminated but occurred on a much slower timescale, similar to the degradation of the other SFKs
98 (20). From this observation we conclude that c-Cbl is solely responsible for the rapid-phase degradation
99 unique to LynA, whereas other E3 ubiquitin ligases can complement c-Cbl to mediate slower-phase
100 SFK degradation. Although activating Syk phosphorylation was increased in Csk$^{AS}$c-Cbl$^{-/-}$ BMDMs
101 relative to Csk$^{AS}$ BMDMs treated with 3-IB-PP1 **(Figure 1E)**, Erk phosphorylation after SFK activation
102 was paradoxically impaired **(Figure 1–figure supplement 1)**, likely due to the loss of the adaptor
103 function of c-Cbl in PI3K signaling (32, 33).

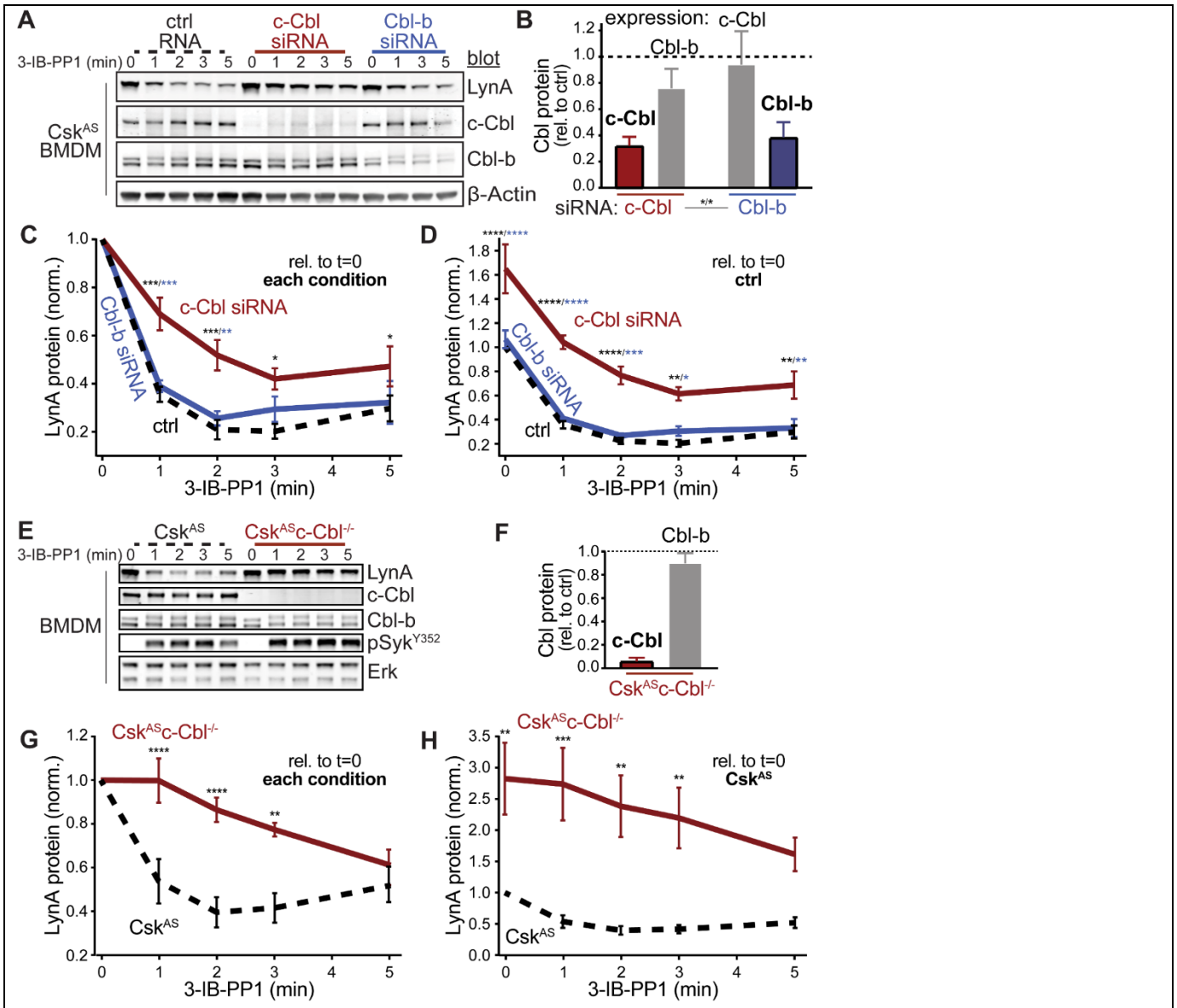


**Figure 1**. **Loss of c-Cbl expression in macrophages leads to steady-state upregulation and delayed degradation of LynA protein. (A)** Immunoblots showing LynA and Cbl protein content of Csk$^{AS}$ BMDMs transfected with non-targeting control RNA (ctrl, black) or siRNA sequences targeting c-Cbl (red) or Cbl-b (blue). After overnight incubation, cells were treated with 3-IB-PP1 for the indicated times; β-actin is shown as a loading control. **(B-D)** Densitometry quantification of relative Cbl and LynA protein levels, corrected for total protein content. Error bars reflect standard error of the mean (SEM), n=3. **(B)** Quantification of c-Cbl and Cbl-b relative to ctrl expression of each (dotted line). Significant differences (Sig.) from two-way ANOVA with Sidak's multiple comparison test (asterisks): [c-Cbl expression: c-Cbl vs. Cbl-b siRNA samples], [Cbl-b expression: c-Cbl vs. Cbl-b siRNA samples]; *

114 P=0.0217-0.0473. **(C-D)** Quantification of LynA relative to t=0 within each siRNA condition **(C)** or the
115 steady-state level in the ctrl **(D)**. Sig. from two-way ANOVA with Tukey's multiple comparison test: [c-
116 Cbl vs. ctrl, black asterisks], [c-Cbl vs. Cbl-b, blue asterisks]; **** P<0.0001, *** P=0.0001-0.0005, **
117 P=0.0015-0.0058, * P=0.0105-0.0451. No significant differences (ns) between other pairs. **(E)**
118 Immunoblots showing LynA and Cbl protein content of $Csk^{AS}$ and $Csk^{AS}$c-$Cbl^{-/-}$ BMDMs treated with 3-
119 IB-PP1; Erk1/2 is shown as a loading control. **(F-H)** Quantification of relative Cbl and LynA protein
120 levels, corrected for total protein content. SEM, n=5. **(F)** Quantification of c-Cbl and Cbl-b in $Csk^{AS}$c-$Cbl^{-}$
121 $^{/-}$ BMDMs relative to expression levels in $Csk^{AS}$ BMDMs (dotted line). **(G-H)** Quantification of LynA
122 relative to t=0 for each genotype **(G)** or the steady-state level in $Csk^{AS}$ BMDMs **(H)**. Sig. from two-way
123 ANOVA with Tukey's multiple comparison test: [$Csk^{AS}$ vs. $Csk^{AS}$c-$Cbl^{-/-}$, asterisks]; **** P<0.0001, ***
124 P=0.0004, ** P=0.0014-0.0048. Paradoxical loss of Erk signaling in c-Cbl-deficient cells is shown in
125 Figure 1–figure supplement 1. Refer to Figure 1–Source Data 1.

126 **A tyrosine residue in the unique-region insert of LynA is required for its rapid degradation**

127 Susceptibility to rapid, activation-induced degradation differentiates LynA from the splice variant LynB
128 and the other macrophage SFKs. Hck, Fgr, LynB, and Fyn (17, 19), are degraded >10-fold more slowly
129 than LynA during 3-IB-PP1 treatment (20) **(Figure 2A)**. Although not expressed in macrophages, Lck is
130 also degraded more slowly than LynA **(Figure 2B)**.

131 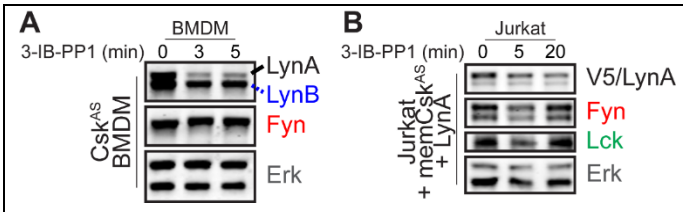


132 **Figure 2. Fyn and Lck are not rapidly degraded upon activation.** Immunoblots and quantification of
133 protein levels of Fyn, Lck, and LynB in 3-IB-PP1-treated $Csk^{AS}$ BMDMs **(A)** and Jurkat cells **(B)**. Total
134 Erk1/2 protein (Erk) is a loading control.

135 As we have been unable to overexpress LynA in BMDMs by transfection, by Amaxa nucleofection, or
136 by lentiviral transduction, we expressed LynA ectopically in Jurkat T cells by transient transfection along
137 with a Cbl construct and a membrane-localized construct of $Csk^{AS}$ ($memCsk^{AS}$) (25), which sensitizes
138 Jurkat cells to 3-IB-PP1 for synchronized SFK activation. As a proof of principle for this model system,
139 we transfected Jurkat cells with wild-type LynA, $memCsk^{AS}$, and empty vector (ctrl), c-Cbl, or Cbl-b
140 plasmid DNA **(Figure 3A)**, which increased c-Cbl expression 3-fold and Cbl-b 25-fold relative to
141 endogenous levels **(Figure 3B)**. Overexpressing one Cbl family member did not affect the abundance
142 of the other. As predicted, c-Cbl overexpression in Jurkat cells increased the rate of LynA degradation
143 (30% depleted after 5 min 3-IB-PP1 treatment in c-Cbl-overexpressing Jurkat cells vs. 10% and 0% in
144 ctrl and Cbl-b-overexpressing cells, respectively) **(Figure 3C)**. This observation is consistent with our
145 siRNA experiments in BMDMs, suggesting that Jurkat cells, which do not normally express Lyn, are
146 capable of supporting rapid, c-Cbl-mediated degradation of LynA.

147 LynB, which lacks a 21 amino-acid insert found in the unique region of LynA **(Figure 3D)**, was less
148 efficiently degraded in c-Cbl-transfected Jurkat cells **(Figure 3E)**, depleted by 10% (LynB) vs. 40%
149 (LynA) from baseline after 5 min 3-IB-PP1 **(Figure 3F)**. These data mirror our findings in $Csk^{AS}$ BMDMs
150 (20) and confirm that the unique sensitivity of LynA to rapid degradation is preserved in the Jurkat
151 model. We hypothesized that the targeting site in LynA must lie within the unique-region insert
152 (residues 23-43) lacking in LynB (34, 35), which contains a tyrosine phosphorylation site (Tyr32) (36), a
153 predicted ubiquitination site (Lys40) (UbPred, 37), and a predicted threonine phosphorylation site
154 (Thr27) (NetPhos 3.1, 38) **(Figure 3D)**.

155 Substituting LynA Tyr32 with either alanine or phenylalanine completely blocked its rapid degradation
156 **(Figure 3E)**, reducing the depletion after 5 min 3-IB-PP1 from 40% (wt) to 10% ($LynA^{Y32A}$) or 8%
157 ($LynA^{Y32F}$) from baseline, levels indistinguishable from LynB **(Figure 3F)**. In contrast, mutation of the
158 predicted ubiquitination ($LynA^{K40R}$) or threonine phosphorylation ($LynA^{T27A}$) sites **(Figure 3E)** did not
159 impair LynA degradation **(Figure 3F)**.

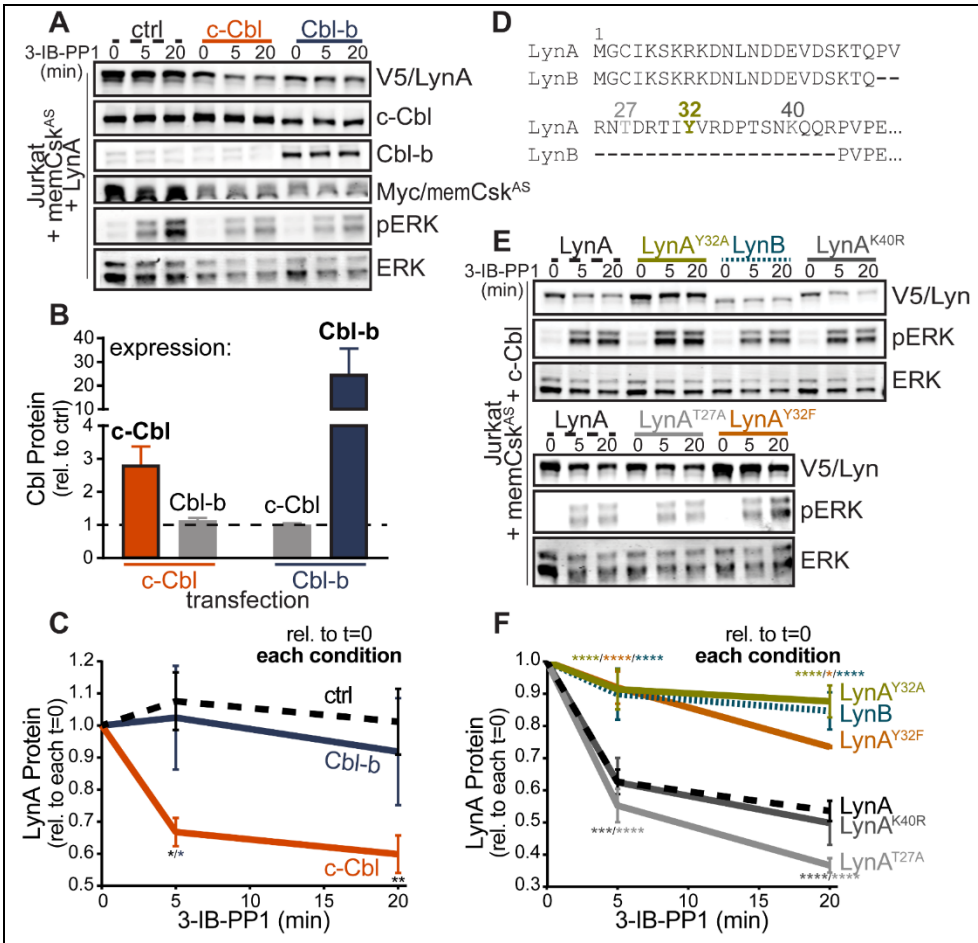


**Figure 3. A unique tyrosine residue is required for activation-induced degradation of LynA. (A)** Immunoblots of Jurkat cells cotransfected with V5-tagged LynA, Myc-tagged memCsk$^{AS}$, and either empty vector (ctrl, black dotted), c-Cbl (orange), or Cbl-b (blue) and treated with 3-IB-PP1. Activating phosphorylation (Thr202/Tyr204) of ERK1/2 (pERK) shows activating signaling, and total ERK1/2 (ERK) shows lane loading. **(B-C)** Quantification of relative Cbl and LynA protein, corrected for total protein content. SEM, n=4. **(B)** Quantification of overexpressed c-Cbl and Cbl-b relative to endogenous (ctrl) levels (dotted line). **(C)** Quantification of LynA protein during 3-IB-PP1 treatment relative to the steady-state level. Sig. from two-way ANOVA with Tukey's multiple comparison test: [c-Cbl vs. ctrl, black asterisks], [c-Cbl vs. Cbl-b, blue asterisks]; ** P=0.0092, * P=0.0270-0.0102. Other pairs ns. **(D)** N-terminal amino-acid sequences of mouse LynA and LynB (34, 35), including the 21 amino-acid unique insert of LynA. Tyrosine 32 (olive), threonine 27 (light gray), and lysine 40 (dark gray) are labeled. **(E)** Immunoblots of 3-IB-PP1-treated Jurkat cells cotransfected with c-Cbl, Myc-tagged memCsk$^{AS}$, and V5-tagged Lyn constructs, including wild-type LynA (black, dashed), LynA$^{Y32A}$ (olive),

174 LynB (teal, dotted), LynA$^{K40R}$ (dark gray), LynA$^{T27A}$ (light gray), or LynA$^{Y32F}$ (orange). **(F)** Quantification
175 of LynA protein levels, corrected for total protein, relative to the steady-state level. SEM, n=7 for LynA,
176 n=4 for LynA$^{Y32A}$ and LynB; n=3 for LynA$^{K40R}$, LynA$^{T27A}$, and LynA$^{Y32F}$. Sig. from two-way ANOVA with
177 Tukey's multiple comparison test: [LynA$^{Y32A}$ vs. LynA, olive asterisks], [LynB vs. LynA, teal asterisks],
178 [LynA$^{Y32F}$ vs. LynA, orange asterisks], [LynA$^{K40R}$ vs. LynA$^{Y32A}$, dark gray asterisks], [LynA$^{T27S}$ vs.
179 LynA$^{Y32A}$, light gray asterisks]; **** P<0.0001, *** P=0.0006, * P=0.0166. ns: [LynA$^{T27S}$ and LynA$^{K40R}$ vs.
180 each other and LynA] and [LynA$^{Y32A}$ and LynA$^{Y32F}$ vs. each other and LynB]. Note: the error bar for
181 LynA$^{Y32F}$ is smaller than the line width. Relative expression levels of LynA variants and LynB are shown
182 in Figure 3–figure supplement 1. Refer to Figure 3–Source Data 1.

183 As in BMDMs, the efficiency of Lyn degradation also affects its steady-state expression in Jurkat cells.
184 LynB is 2- and LynA$^{Y32A}$ 3-fold more highly expressed than wild-type LynA, LynA$^{K40R}$, or LynA$^{T27A}$ in
185 resting cells, resulting in 3- to 4-fold more protein remaining after 20 min treatment with 3-IB-PP1
186 **(Figure 3–figure supplement 1)**. Overall, we conclude that the unique tyrosine residue in the LynA
187 insert, a known site of tyrosine phosphorylation (36), is the recognition site for rapid, c-Cbl-mediated
188 degradation, and that this mechanism determines the half-life of activated LynA protein within an ITAM
189 signaling complex and tunes the steady-state expression of LynA protein. This suggests that c-Cbl-
190 mediated regulation of steady-state LynA protein levels occurs as a direct effect of c-Cbl protein activity
191 rather than merely a transcriptional feedback effect.

192 **LynA kinase activity is required for its rapid degradation**

193 SFK activation is a requirement for rapid degradation of LynA protein in BMDMs (20), but whether this
194 is direct effect of the LynA kinase itself or initiated by feedback from downstream signaling proteins has
195 been unclear. To investigate the role of LynA kinase activity in its degradation, we tested two
196 functionally impaired LynA constructs. First, we introduced a lysine residue in place of an activation-
197 loop threonine (T410K, c-Src residue 429 (39)) to disrupt substrate recognition (40). Second, we
198 introduced a phenylalanine residue in place of the activation-loop tyrosine, a known site of interaction

199 between the phosphotyrosine binding (PTB) domain of c-Cbl and Src (41) and the key

200 autophosphorylation site that stabilizes the active state (27, 42) (Y397F, c-Src residue 416).

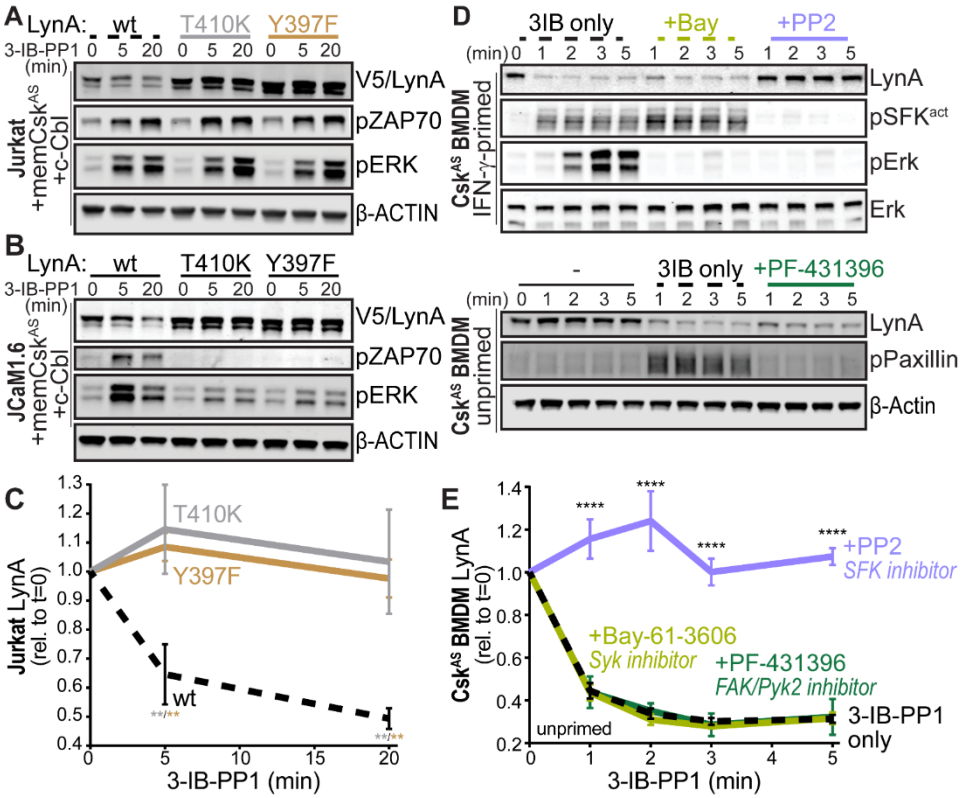


201

202 **Figure 4. SFK catalytic activity is required for rapid degradation of LynA. (A)** Immunoblots

203 showing ectopic expression of wild-type (wt, black dotted), substrate-binding-impaired (T410K, gray), or

204 activation-loop-mutated (Y397F, orange) V5-tagged LynA protein coexpressed in Jurkat cells with

205 memCsk$^{AS}$ and c-Cbl and treated with 3-IB-PP1. pERK is shown as a control for 3-IB-PP1 treatment. β-

206 actin reflects lane loading. **(B)** Overexpression of wt and variants of LynA in JCaM1.6 cells. ZAP70

207 (Y319) and ERK are phosphorylated as a consequence of SFK activation. **(C)** Quantification of LynA

208 protein in transfected Jurkat cells during 3-IB-PP1 treatment, corrected for total protein, relative to the

209 steady-state level for each variant. SEM, n=3. Sig. from two-way ANOVA with Tukey's multiple

210 comparison test: [T410K vs. wt, gray asterisks], [Y397F vs. wt, orange asterisks]; ** P=0.0015-0.0083.

211 Other pairs ns. **(D)** Immunoblots showing expression of endogenous LynA protein in Csk$^{AS}$ BMDMs

212 treated with 3-IB-PP1 (3IB only, black dotted) or with 3-IB-PP1 plus the Syk inhibitor Bay-61-3606 (Bay,

213 light olive), the SFK inhibitor PP2 (light purple), or the FAK/Pyk2 inhibitor PF-431396 (green).

214 Phosphorylated SFK activation loop Tyr416 (pSFK$^{act}$), Erk1/2 (pErk), and Paxillin Tyr118 (pPaxillin) are
215 shown as controls for inhibitor function; β-actin and Erk are shown as loading controls. **(E)**
216 Quantification of LynA protein during 3-IB-PP1 treatment, corrected for total protein, relative to the
217 steady-state level. SEM, n=3. Sig. from two-way ANOVA with Tukey's multiple comparison test: [+PP2
218 vs. 3IB only, asterisks]; **** P<0.0001. Other pairs ns. Refer to Figure 4–Source Data 1.

219 In untransfected Jurkat cells ERK1/2 is phosphorylated downstream of the endogenous SFKs Lck (43,
220 44) and Fyn (45), which are activated following treatment with 3-IB-PP1 (25). Since the endogenous
221 kinases are not disrupted by substitutions in transfected LynA, ERK1/2 continues to be efficiently
222 phosphorylated in cells transfected with LynA T410K or Y397F **(Figure 4A)**. In JCaM1.6 cells, an Lck-
223 deficient Jurkat strain (43, 46), ERK1/2 phosphorylation depended on transfected LynA and reflected
224 the functional impairment of LynA T410K and Y397F **(Figure 4B)**. As reported previously, Fyn activity
225 in the absence of Lck cannot mediate ERK1/2 phosphorylation (43).

226 Functional LynA kinase was required for c-Cbl-mediated degradation in Jurkat cells. While wild-type
227 LynA protein was 50% depleted after 20 min of 3-IB-PP1 treatment, degradation of either LynA T410K
228 or Y397F was undetectable **(Figure 4C)**. The dependence on LynA kinase function was evident in both
229 Lck- and Fyn-expressing Jurkat cells **(Figure 4A)** and Lck-deficient JCaM1.6 cells **(Figure 4B)**,
230 indicating that, in this system, the other activated SFKs could not target LynA in trans to induce c-Cbl-
231 mediated degradation. We do not yet know whether the unique insert of LynA is a substrate for the
232 other macrophage SFKs, but the peptide containing Tyr32 is a predicted SFK substrate (NetPhos 3.1,
233 38).

234 In macrophages and other hematopoietic cells the SFKs are the first kinases to be activated upon
235 antigen receptor engagement, phosphorylating intracellular ITAMs, ITAM-associated Syk or Zap70, and
236 integrin-associated FAK or Pyk2 (4, 47). We have reported that Syk and FAK are phosphorylated on
237 activating tyrosine residues in Csk$^{AS}$ BMDMs treated with 3-IB-PP1 (20). To test whether these
238 downstream kinases might participate in negative feedback leading to LynA degradation, we treated

239 Csk$^{AS}$ macrophages with competitive inhibitors of Syk (48), FAK/Pyk2 (49), or the SFKs themselves
240 (50) in combination with 3-IB-PP1. As controls for on-target effects, we demonstrated that Erk1/2 and
241 SFK activation-loop phosphorylation was blocked in samples cotreated with the pan-SFK inhibitor PP2,
242 that Erk1/2 but not SFK activation-loop phosphorylation was blocked in samples cotreated with the Syk
243 inhibitor BAY-61-3606, and that Paxillin phosphorylation was blocked in samples cotreated with the
244 FAK/Pyk2 inhibitor PF-431396 **(Figure 4D)**. As with genetically impairing LynA kinase function,
245 inhibiting SFK activity with PP2 abrogated LynA degradation **(Figure 4D-E)**. In contrast, LynA
246 degradation in BMDMs was unaffected by cotreatment with BAY-61-3606 or PF-431396. Together
247 these data suggest that Syk and FAK/Pyk2 (and any off-target effects of BAY-61-3606 and PF-431396)
248 do not participate in a larger negative-feedback process, suggesting that LynA might target itself
249 directly through Tyr32 in cis or trans. Interestingly, since the T-cell SFKs Lck and Fyn cannot effect
250 LynA degradation in trans, this feedback process could be limited to a kinase effect in cis or to another
251 macrophage-expressed Src family member. This tight feedback circuit could explain the strikingly fast
252 kinetics of LynA degradation.

253 **Differential Cbl expression tunes LynA protein levels and signaling responses in macrophages**
254 **and mast cells**

255 Analysis of data from the Immunological Genome Project shows that expression levels of Lyn and c-Cbl
256 RNA are differentially regulated across different cell types. Mast cells, for instance, express very low
257 levels of c-Cbl mRNA **(Figure 5)** (51, 52), which corresponds to a low level of c-Cbl protein expression
258 (53). Cbl-b mRNA, in contrast, is abundant in mast cells.

259 As in macrophages, Lyn is a key regulator of mast-cell ITAM signaling (54), but the effect of disparate
260 Cbl-family expression on LynA in the two cell types remains unknown. We generated bone-marrow-
261 derived mast cells from Csk$^{AS}$ mice (hereafter referred to as “mast cells”) and performed surface marker
262 analysis as we had done already for BMDMs (20). Csk$^{AS}$ mast cells were homogenous in their
263 expression of traditional mast-cell markers FcεR1α and c-Kit (CD117) (55) **(Figure 6A)**.

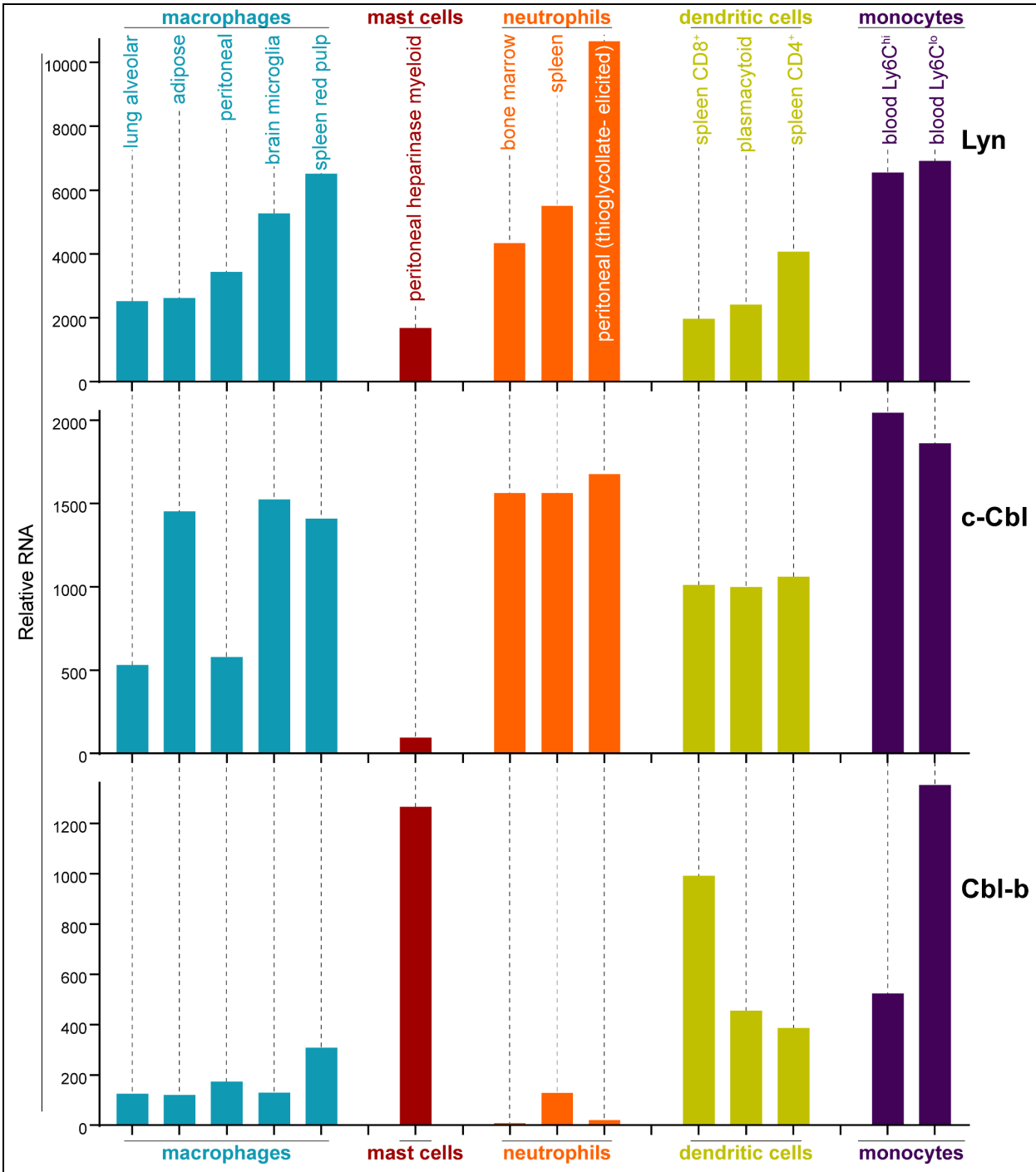


**Figure 5. LynA, c-Cbl, and Cbl-b mRNAs are regulated differentially in myeloid cells.** Mouse RNAseq data were derived from the Immunological Genome Project (ImmGen, http://rstats.immgen.org/Skyline/skyline.html, 51, 52). RNA levels of Lyn, c-Cbl, and Cbl-b are shown for macrophages, mast cells, neutrophils, dendritic cells, and blood monocytes. Refer to Figure 5–Source Data 1.

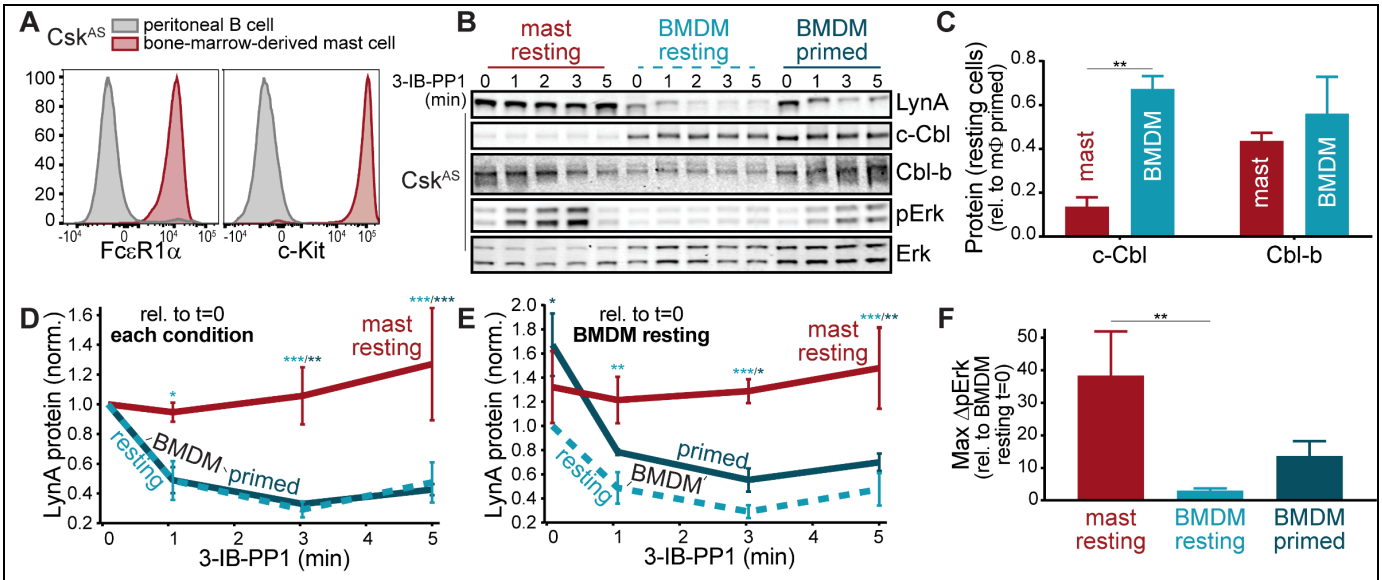


**Figure 6. c-Cbl expression correlates with LynA protein levels and pathway activation in macrophages and mast cells. (A)** Flow cytometry plots showing surface expression of the mast-cell markers FcεR1α and c-Kit (CD117) in Csk$^{AS}$ bone-marrow-derived mast cells compared to a peritoneal B-cell control. **(B)** Immunoblots of Csk$^{AS}$ bone-marrow-derived mast cells (mast resting, red) and BMDMs after resting (light teal) or IFN-γ priming (dark teal). LynA, c-Cbl, Cbl-b, and pErk1/2 are shown; total Erk1/2 reflects lane loading. **(C)** Quantification of c-Cbl and Cbl-b protein in mast cells and macrophages, corrected for total protein, relative to the level in primed macrophages (mΦ). SEM, n=3. Sig. from one-way ANOVA with Sidak multiple comparison test: [mast vs. BMDM resting, asterisk]; ** P= 0.0035. Others pairs ns. **(D-E)** Quantification of LynA, corrected for total protein, relative to the steady-state level in each cell condition **(D)** or in resting BMDMs at t=0 **(E)**. SEM, n=3 for mast cells and primed BMDMs, 4 for resting BMDMs. Sig. from two-way ANOVA with Tukey's multiple comparison test: [mast vs. BMDM resting, light teal asterisks], [mast vs. BMDM primed, dark teal asterisks]; *** P=0.0004-0.0008, ** P=0.0025-0.0088, * P=0.0134-0.0466. Other pairs ns. **(F)** Quantification of the maximum increase in pErk1/2 over the first 5 min of 3-IB-PP1 treatment, corrected for total Erk1/2 protein, relative to the level in resting BMDMs at t=0. SEM, n=3 for mast cells, 5 for resting BMDMs, and 4 for primed BMDMs. Sig. from one-way ANOVA with Tukey's multiple comparison test: [mast vs. BMDM resting, light teal asterisks]; ** P= 0.0085. Others pairs ns. Refer to Figure 6–Source Data 1.

288 We then used immunoblotting to compare the expression of Cbl and LynA protein in Csk$^{AS}$ mast cells
289 and BMDMs **(Figure 6B)** and found that mast cells express very little c-Cbl (20% of the level in resting
290 macrophages) and relatively high levels of Cbl-b (80% of the level in resting macrophages) **(Figure**
291 **6C)**. Strikingly, low c-Cbl expression was accompanied by a complete resistance of LynA to
292 degradation in the first 5 min of 3-IB-PP1 treatment **(Figure 6D)** and an increase in steady-state
293 expression of LynA (30% higher than in resting BMDMs) **(Figure 6E)**, resulting in 3-4x more LynA
294 protein in mast cells than in resting BMDMs and 2x more than in primed BMDMs between 3 and 5 min
295 of 3-IB-PP1 treatment. Mast cells also had a stronger signaling response to 3-IB-PP1. Although the
296 kinetics of Erk phosphorylation in mast cells varied among experiments, the fold increase in pErk1/2 in
297 the first 5 min of 3-IB-PP1 treatment was consistently higher than in macrophages, even primed
298 BMDMs (40x pErk increase in mast cells compared with 14x in primed BMDMs and no significant
299 increase in resting BMDMs) **(Figure 6F)**. We therefore conclude that c-Cbl expression tunes the
300 steady-state expression of LynA protein and the cell's ability to target LynA for rapid degradation upon
301 activation. Since mast cells are less dependent on c-Cbl for positive signaling, long-lived LynA
302 potentiates a strong response to 3-IB-PP1. Thus mast cells bypass the LynA signaling checkpoint by
303 maintaining low levels of c-Cbl and therefore high levels of activated LynA.

## 304 Discussion

305 Both c-Cbl and Cbl-b negatively regulate ITAM signaling, recognizing activated signaling proteins via
306 PTB binding to activating phosphotyrosine sites. Cbl-mediated polyubiquitination leads to protein
307 degradation via the lysosome and proteasome (56). Cbl-family ligases must in turn be tightly regulated
308 to prevent hyperresponsive or aberrant signaling while maintaining proper pathogen clearance (57).
309 Although highly homologous, c-Cbl and Cbl-b target different subsets of signaling proteins for
310 degradation (58, 59), with c-Cbl targeting the SFKs, including Lyn (60, 61), and Cbl-b interacting with
311 ITAM-coupled receptors and other kinases (31, 53, 57). c-Cbl is thought to interact with active SFKs
312 through the SFK activation-loop phosphotyrosine residue, which binds the c-Cbl PTB domain (62), and
313 through the SFK SH3 domain, which binds the c-Cbl PXXP motifs (63). In this paper we report a new

314 mode of recognition specific to LynA. Although LynA and LynB have identical activation kinetics and
315 activation-loop and SH3-domain sequences, LynB is degraded 10-fold more slowly in macrophages
316 treated with 3-IB-PP1 (20). This rapid degradation profile is unique among the SFKs we have tested
317 (LynB, HckA, HckB, Fgr (20), and Fyn in BMDMs and Lck and Fyn in Jurkat cells). By exploiting the
318 similarity between LynA and LynB, we conclude that, while activation-loop phosphorylation and SH3-
319 domain interactions mediate slower-phase targeting by c-Cbl and other E3 ligases, rapid degradation of
320 LynA is triggered by an interaction unique to its insert region.

321 A single tyrosine residue (Tyr32) peculiar to its unique region marks activated LynA for rapid
322 degradation. This phenomenon is easily observed upon bulk SFK activation by 3-IB-PP1 but also
323 affects the steady-state level of LynA protein, likely due to the degradation of basally active LynA over
324 time. Phosphorylation of LynA Tyr32 has been observed in neuroblastoma cell lines upon receptor-
325 tyrosine-kinase activation (64). Further, in epidermoid carcinoma (A431) cells and breast tumor
326 samples LynA Tyr32 is phosphorylated by the epidermal growth factor receptor (EGFR), allowing it to
327 phosphorylate MCM-7 and stimulate cell proliferation (36). In macrophages this potentially positive-
328 regulatory function of Tyr32 paradoxically causes LynA to trigger its own c-Cbl-mediated degradation,
329 underlying its function as a rheostat in the LynA checkpoint. We can speculate about two possible
330 mechanisms. First, by analogy to a similarly situated but non-homologous transautophosphorylation
331 site in Hck ($Tyr^{29}$) (65), LynA phospho-Tyr32 may be directly activating. The unique regions of LynA
332 and LynB make distinct SH3-domain contacts (66), and phospho-Tyr32 could alter these interactions.
333 Hyperactivated LynA could then efficiently phosphorylate and activate nearby or pre-complexed c-Cbl,
334 triggering its own degradation more aggressively than do the other SFKs. Alternatively, phospho-Tyr32
335 could directly or indirectly serve as a docking site for c-Cbl, constituting a unique interaction site to
336 efficiently recruit its degradation machinery. Bolstering this hypothesis is a published study showing that
337 the interactome of $LynA^{Y32F}$ transfected into mammary adenocarcinoma (MDA-MB-231) cells more
338 closely resembles the interactome of wild-type LynA than LynB, but some LynA interactions are lost
339 (67). It is also possible that LynA Tyr32 is not phosphorylated, but is required for an allosteric

340 intramolecular interaction or docking of interacting proteins.

341 We have shown that SFK activity is required for LynA degradation, and LynA Tyr32 is a predicted
342 substrate for Hck (NetPhos 3.1, 38) in addition to EGFR. It is therefore tempting to speculate that LynA
343 Tyr32 is a site of autophosphorylation, since the SFKs Lck and Fyn cannot mediate the degradation of
344 kinase-impaired LynA in trans. On the other hand, we have shown that LynA and LynB are activation-
345 loop phosphorylated 20x more quickly than Hck and Fgr in response to 3-IB-PP1 (20), and it is possible
346 that this delay could function as a timer, allowing a rapid burst of LynA activation with a short half-life,
347 either globally (in the case of 3-IB-PP1 treatment) or at the single-molecule scale within a phagocytic
348 synapse.

349 LynA and LynB have been reported to interact with different subsets of proteins in mast cells and in
350 triple-negative breast cancer cells, with LynA signaling via ITAM (18), cytoskeletal, and proliferative (67)
351 pathways and LynB initiating negative feedback via ITIMs and phosphatases (18). In mammary
352 epithelial cells the ratio of LynA and LynB is actively regulated by Epithelial Splicing Regulatory Protein
353 1 (ESRP1), with LynA-upregulated tumors having the more invasive phenotype (67). The positive-
354 regulatory roles reported for LynA in mast and tumor cells complements our own observations that
355 LynA degradation can block macrophage signaling through the Erk, Akt, and NFAT pathways, which
356 cannot be complemented by active LynB (20).

357 Aberrant activation driven by ITAM signaling pathways in macrophages is a known driver of
358 autoimmune and inflammatory disease, with activated macrophages accumulating in chronically
359 inflamed tissues in the absence of an active infection (68). Regulation of LynA protein expression and
360 deactivation kinetics by c-Cbl, could, via the LynA checkpoint, help to prevent the initiation of
361 pathological signaling. The threshold for macrophage activation is modifiable by changes to their local
362 environment. For example, IFN-γ and LPS polarize macrophages for a pro-inflammatory response,
363 whereas IL-4 and IL-13 polarize macrophages for tissue repair (i.e. collagen deposition) and
364 inflammatory resolution (69, 70). We have reported that IFN-γ decreases the macrophage signaling

365 threshold in part by increasing the expression of LynA (20). Dynamic changes in SFK and c-Cbl levels
366 could modulate the macrophage activation threshold, ensuring that macrophages respond appropriately
367 during times of infection (low threshold) and limiting aberrant activation in response to cellular debris
368 and small-scale antibody complexes during inflammatory resolution (high threshold).

369 Like macrophages, mast cells reside in nearly every bodily tissue and perform environment-specific
370 functions in addition to sensing non-self (69, 71). While macrophages have distinct anti-inflammatory
371 roles as professional phagocytes in the silent clearance of apoptotic cells and agents of wound healing,
372 mast cells are constitutively primed for ITAM-induced triggering, releasing preformed granules that
373 contain inflammatory cytokines, chemokines, prostaglandins, and proteases. Pursuant to these differing
374 functions, macrophages continuously gauge ITAM ligand valency (*i.e.* particle size) and have a
375 relatively high basal threshold for inflammatory activation (5, 20), while mast cells can be triggered by
376 small-scale receptor clustering induced by low-valency or even monovalent FcεR-IgE-allergen
377 complexes (21, 22). One striking difference between the macrophage and mast-cell ITAM regulatory
378 machinery is that mast cells express almost no c-Cbl. In spite of low reported mRNA levels (ImmGen,
379 51, 52), mast cells constitutively express a high level of LynA protein, likely due to impaired steady-
380 state degradation of basally active LynA. Furthermore, LynA is not degraded upon activation and 3-IB-
381 PP1 triggers a stronger Erk phosphorylation response in the absence of ITAM-receptor ligation in
382 resting mast cells than in resting macrophages.

383 Overall, we describe a model in which regulation of LynA and c-Cbl levels helps to determine an
384 immune cell's potential for inflammatory ITAM signaling. Regulated degradation tunes down the LynA
385 rheostat, blocking cell signaling via the LynA checkpoint at low cellular doses of LynA and overriding
386 the LynA checkpoint at higher doses. In macrophages, this occurs on a continuum where LynA dose is
387 highest in M1-polarized cells but still susceptible to rapid degradation by c-Cbl. Mast cells express
388 almost no c-Cbl and maintain high levels of LynA at steady state and over time, consistent with
389 permissive signaling in the absence of large-scale ITAM receptor clustering nucleated by multivalent
390 receptor ligation. Appropriate regulation of immune receptor thresholds is critical for maintaining the

391 function of innate immune cells; threshold dysregulation can lead to chronic feedback loops that drive
392 inflammatory signaling in autoimmune disease and conversely tumor-supporting immunosuppressive
393 signaling (68). Elucidating the mechanisms by which the LynA checkpoint is regulated may allow us to
394 tune immune-cell sensitivity and reprogram pathological cells without causing immunodeficiency.

## 395 Materials and Methods

### 396 Mice

397 C57BL/6-derived *Csk*$^{AS}$ mice are hemizygous for the *Csk*$^{AS}$ BAC transgene on a *Csk*$^{-/-}$ background, as
398 described previously (20, 26). Due to sterility of c-Cbl$^{-/-}$ male mice, we were not able to produce a
399 sustained lineage of *Csk*$^{AS}$*Cbl*$^{-/-}$ mice, but we obtained three individuals by crossing *c-Cbl*$^{-/-}$ female mice
400 from E. Peterson (University of Minnesota) (72) with *Csk*$^{+/-}$ (26) and *Csk*$^{AS}$ male mice from our colony
401 and then crossing *Cbl*$^{+/-}$*Csk*$^{+/-}$ *with Cbl*$^{+/-}$*Csk*$^{AS}$ mice. All mice were housed in specific pathogen-free
402 conditions and genotyped using real-time PCR (Transnetyx, Inc., Memphis, TN).

### 403 Jurkat cell lines and transfection

404 The Jurkat T-cell strains E6-1 (“wild-type”) (73) and JCaM1.6 (Lck-deficient) (43, 46) were gifts from the
405 laboratories of A. Weiss (University of California, San Francisco) and Y. Shimizu (University of
406 Minnesota), respectively. Jurkat cell lines were cultured in RPMI-1640 medium supplemented with 5%
407 fetal calf serum (Omega Scientific, Inc., Tarzana, CA) and 2 mM glutamine, penicillin and streptomycin
408 (Sigma-Aldrich, St. Louis, MO) as described previously *(74).* Jurkat and JCaM1.6 cells were transiently
409 transfected via electroporation, as described previously (74). Briefly, cells were grown overnight in
410 antibiotic-free RPMI-1640 medium supplemented with 10% fetal bovine serum (Omega Scientific) and 2
411 mM glutamine (RPMI10). Batches of 15 M cells were resuspended in RPMI10 with 15 µg plasmid DNA
412 per construct. Cells were rested 20 min, electroporated 285 V/10 ms in a BTX square-wave
413 electroporator (Harvard Apparatus, Holliston, MA), resuspended in 10 mL RPMI10, and allowed to
414 recover overnight. One million live cells were then resuspended in phosphate-buffered saline, rested for

415 30 min at 37°C, and stimulated.

416 **DNA constructs and mutagenesis**

417 Plasmids containing V5+His-tagged mouse LynA and LynB were gifts from J. Rivera/R. Suzuki
418 (National Institutes of Health) (18). Myc-tagged mouse memCsk$^{AS}$ (also referred to as Lck$_{11}$-Csk$^{AS}$) (25)
419 and Xpress-tagged human c-Cbl and Cbl-b (75) were gifts from A. Weiss (University of California, San
420 Francisco). Site-directed mutagenesis was performed using QuikChange Lightning (Agilent
421 Technologies, Santa Clara, CA). Sequences of all constructs were verified by Sanger sequencing
422 (GENEWIZ, South Plainfield, NJ).

423 **Preparation and flow cytometry of myeloid cells**

424 BMDMs were prepared using standard methods (76). Briefly, bone marrow was extracted from femura
425 and tibiae of mice aged 6-8-weeks. After hypotonic lysis of erythrocytes, BMDMs were derived on
426 untreated plastic plates (BD Falcon, Sigma-Aldrich) by culturing in Dulbecco's Modified Eagle Medium
427 (DMEM, Corning Cellgro, Corning, NY) containing approximately 10% heat-inactivated fetal calf serum
428 (Omega Scientific), 0.11 mg/ml sodium pyruvate (Corning), 2 mM penicillin/streptomycin/L-glutamine
429 (Sigma-Aldrich), and 10% CMG-14-12-cell-conditioned medium as a source of M-CSF (77). After 6 or 7
430 days cells were resuspended in enzyme-free EDTA buffer and replated in untreated 6-well plates (BD
431 Falcon, Sigma-Aldrich) at 1 M cells per well in unconditioned medium with or without priming in 25 U
432 IFN-γ (PeproTech, Rocky Hill, NJ). Bone-marrow-derived mast cells were prepared as described
433 previously (55), as above except for the substitution of 10 ng/ml IL-3 (PeproTech) for CMG-14-12-
434 conditoned medium. After 5 weeks, cells were subjected to flow-cytometry analysis (LSRFortessa,
435 Becton Dickinson, Franklin Lakes, NJ) and found to be uniformly positive for FcεRIα (Mar-1, FITC-
436 labeled, #134305) and c-Kit (2B8, APC-labeled, #105811), both from BioLegend (San Diego, CA). Cells
437 were rested or primed overnight before stimulation.

438 **siRNA knockdown**

439 The siRNA sequence for knockdown of mouse c-Cbl was adapted from human siRNA. Cbl-b siRNA
440 was designed using the Integrated DNA Technologies double-stranded siRNA design tools (IDT,
441 Skokie, IL). Control double-stranded RNA from IDT was not predicted to be complementary to any
442 sequence in human, mouse, or rat transcriptomes. 2 M BMDMs in 100 μL opti-MEM (ThermoFisher,
443 Waltham, MA) were transfected with 1 μM siRNA via electroporation at 400 V/10 ms using a BTX
444 square-wave electroporator. Cells were then plated on 150 mm untreated cell culture dishes and rested
445 in 10 mL DMEM-10 for 30 min before adding 10 mL DMEM-10 supplemented with 10% CMG-14-12-
446 cell-conditioned medium as a source of M-CSF. Transfections were pooled from several cuvettes to
447 obtain enough cells for several stimulation conditions. After 24 h cells were resuspended in enzyme-
448 free EDTA buffer and replated in untreated 6-well plates (BD Falcon, Sigma-Aldrich) at 1 M cells per
449 well in unconditioned medium. Cells were used 48 h after transfection.

450 **Cell stimulation**

451 BMDM stimulations have been described previously (20). After resting as described above, 1 M live
452 Jurkat cells, mast cells, or adherent BMDMs were treated at 37°C in DMEM (myeloid cells) or PBS
453 (Jurkat cells) with 10 μM 3-IB-PP1, a gift from K. Shokat (University of California, San Francisco).
454 Signaling reactions were quenched by placing on ice and lysing cells in sodium dodecyl sulfate (SDS)
455 buffer (128 mM Tris base, 10% glycerol, 4% SDS, 50 mM dithiothreitol, pH 6.8). Whole-cell lysates
456 were prepared for immunoblotting by sonicating with a Bioruptor (Diagenode, Inc., Denville, NJ) for 3
457 min and boiling for 15 min.

458 **Antibodies and immunoblotting**

459 After sample preparation, 0.25 M cell equivalents were run on each lane of a 7% NuPage Tris-Acetate
460 gel (Invitrogen, Carlsbad, CA) and then transferred to an Immobilon-FL PVDF membrane (EMD
461 Millipore, Burlington, MA). REVERT Total Protein Stain was used according to the standard protocol to
462 quantify lane loading. After destaining, membranes were then treated with Odyssey® Blocking Buffer
463 (TBS) for at least 1 h. Blotting was performed using standard procedures, and blots were imaged on an

464 Odyssey CLx near-infrared imager (LI-COR Biosciences, Lincoln, NE). Antibodies for immunoblotting
465 were purchased from Cell Signaling Technology (Danvers, MA), ProMab Biotechnologies (Richmond,
466 CA), Thermo Fisher Scientific (Waltham, MA), LifeSpan Biosciences (Seattle, WA), Abcam (Cambridge,
467 UK), and LI-COR Biosciences as follows:

| Antibody | Source and Catalog No. |
|---|---|
| β-Actin (8H10D10) | Cell Signaling 3700 |
| c-Cbl (D4E10) | Cell Signaling 8447 |
| Cbl-b (D3C12) | Cell Signaling 9498 |
| pErk1/2 (phosphoThr$^{202}$/phosphoTyr$^{204}$, D13.14.4E) | Cell Signaling 4370 |
| Erk1/2 (3A7) | Cell Signaling 9107 |
| Fyn | Cell Signaling 4023 |
| Lck (D88) XP(R) | Cell Signaling 2984 |
| LynA (C13F9) | Cell Signaling 2796 |
| LynA + LynB (Lyn-01) | Abcam ab1890 |
| Myc (9B11) | Cell Signaling 2276 |
| pPaxillin (phosphoTyr$^{118}$) | Cell Signaling 2541 |
| pSFK$^{act}$ (phosphoTyr$^{416}$) | Cell Signaling 2101 |
| pZAP70/pSyk (phosphoTyr$^{319(Zap)/352(Syk)}$, 65E4) | Cell Signaling 2717 |
| V5 (D3H8Q) | Cell Signaling 13202 |
| Donkey anti-rabbit IgG 800CW | LI-COR 925-32213 |
| Donkey anti-rabbit IgG 680LT | LI-COR 925-68023 |
| Donkey anti-mouse IgG 800CW | LI-COR 925-32212 |
| Donkey anti-mouse IgG 680LT | LI-COR 925-68022 |

468 **Quantification, statistics, and image processing**

469 Immunoblots were analyzed by densitometry from ImageStudio software (LI-COR Biosciences). Images
470 were background-subtracted, and bands of the appropriate molecular weight were demarcated and
471 analyzed for each gel lane. Each value was corrected for the total lane protein content (REVERT stain,
472 above). Data were further normalized to a control condition to show relative changes in protein content.
473 Where phosphoproteins were quantified, these were corrected for the total amount of the individual
474 protein, rather than whole-lane protein content. For all figures, n values are biological replicates,
475 reflecting independent experiments from different batches of cells, stimulus preparations, and
476 experimental workflows. Statistical analyses were performed using Prism Software (Graphpad, La Jolla,
477 CA). Significance was assessed using one- or two-way ANOVA analysis with Tukey's or Sidak
478 correction for multiple comparisons as indicated in the figure legends, with analysis of the mean at each
479 time point or condition. Error bars in each figure represent standard errors of the mean from at least

480 three independent experiments. Asterisks reflect specified P-values. Figures were further prepared
481 using Adobe Creative Cloud software (San Jose, CA). Where appropriate, images were optimized by
482 applying brightness/contrast changes to the whole image. No gamma correction was used. Images
483 were only rotated after densitometry analysis was completed.

## 484 References


485 1. Guilliams M, Bruhns P, Saeys Y, Hammad H, Lambrecht BN. The function of Fcgamma
486 receptors in dendritic cells and macrophages. Nat Rev Immunol. 2014;14(2):94-108.

487 2. Brown GD. Dectin-1: a signalling non-TLR pattern-recognition receptor. Nat Rev Immunol.
488 2006;6(1):33-43.

489 3. Deng Z, Ma S, Zhou H, Zang A, Fang Y, Li T, et al. Tyrosine phosphatase SHP-2 mediates C-
490 type lectin receptor-induced activation of the kinase Syk and anti-fungal TH17 responses. Nat Immunol.
491 2015;16(6):642-52.

492 4. Lowell CA. Src-family and Syk kinases in activating and inhibitory pathways in innate immune
493 cells: signaling cross talk. Cold Spring Harb Perspect Biol. 2011;3(3).

494 5. Goodridge HS, Reyes CN, Becker CA, Katsumoto TR, Ma J, Wolf AJ, et al. Activation of the
495 innate immune receptor Dectin-1 upon formation of a 'phagocytic synapse'. Nature.
496 2011;472(7344):471-5.

497 6. Takai T. Roles of Fc receptors in autoimmunity. Nat Rev Immunol. 2002;2(8):580-92.

498 7. Sondermann P. The FcgammaR/IgG Interaction as Target for the Treatment of Autoimmune
499 Diseases. J Clin Immunol. 2016;36 Suppl 1:95-9.

500 8. Chiffoleau E. C-Type Lectin-Like Receptors As Emerging Orchestrators of Sterile Inflammation
501 Represent Potential Therapeutic Targets. Front Immunol. 2018;9:227.

502 9. Freeman SA, Goyette J, Furuya W, Woods EC, Bertozzi CR, Bergmeier W, et al. Integrins Form
503 an Expanding Diffusional Barrier that Coordinates Phagocytosis. Cell. 2016;164(1-2):128-40.

504 10. Bakalar MH, Joffe AM, Schmid EM, Son S, Podolski M, Fletcher DA. Size-Dependent
505 Segregation Controls Macrophage Phagocytosis of Antibody-Opsonized Targets. Cell.
506 2018;174(1):131-42 e13.

507 11. Jaumouille V, Farkash Y, Jaqaman K, Das R, Lowell CA, Grinstein S. Actin cytoskeleton
508 reorganization by Syk regulates Fcgamma receptor responsiveness by increasing its lateral mobility
509 and clustering. Dev Cell. 2014;29(5):534-46.

510 12. Abram CL, Lowell CA. The diverse functions of Src family kinases in macrophages. Front
511 Biosci. 2008;13:4426-50.

512 13. Hamerman JA, Lanier LL. Inhibition of immune responses by ITAM-bearing receptors. Sci
513 STKE. 2006;2006(320):re1.

514 14. Hamerman JA, Ni M, Killebrew JR, Chu CL, Lowell CA. The expanding roles of ITAM adapters
515 FcRgamma and DAP12 in myeloid cells. Immunol Rev. 2009;232(1):42-58.

516 15. Lutz-Nicoladoni C, Wolf D, Sopper S. Modulation of Immune Cell Functions by the E3 Ligase
517 Cbl-b. Front Oncol. 2015;5:58.

518 16. Liyasova MS, Ma K, Lipkowitz S. Molecular pathways: cbl proteins in tumorigenesis and
519 antitumor immunity-opportunities for cancer treatment. Clin Cancer Res. 2015;21(8):1789-94.

520 17. Mkaddem SB, Murua A, Flament H, Titeca-Beauport D, Bounaix C, Danelli L, et al. Lyn and Fyn
521 function as molecular switches that control immunoreceptors to direct homeostasis or inflammation. Nat
522 Commun. 2017;8(1):246.

523 18. Alvarez-Errico D, Yamashita Y, Suzuki R, Odom S, Furumoto Y, Yamashita T, et al. Functional
524 analysis of Lyn kinase A and B isoforms reveals redundant and distinct roles in Fc epsilon RI-
525 dependent mast cell activation. J Immunol. 2010;184(9):5000-8.

526 19. Scapini P, Pereira S, Zhang H, Lowell CA. Multiple roles of Lyn kinase in myeloid cell signaling
527 and function. Immunol Rev. 2009;228(1):23-40.

528 20. Freedman TS, Tan YX, Skrzypczynska KM, Manz BN, Sjaastad FV, Goodridge HS, et al. LynA
529 regulates an inflammation-sensitive signaling checkpoint in macrophages. Elife. 2015;4.

530 21. Andrews NL, Pfeiffer JR, Martinez AM, Haaland DM, Davis RW, Kawakami T, et al. Small,
531 mobile FcepsilonRI receptor aggregates are signaling competent. Immunity. 2009;31(3):469-79.

532 22. Felce JH, Sezgin E, Wane M, Brouwer H, Dustin ML, Eggeling C, et al. CD45 exclusion- and
533 cross-linking-based receptor signaling together broaden FcepsilonRI reactivity. Sci Signal.
534 2018;11(561).

535 23. Okuzumi T, Ducker GS, Zhang C, Aizenstein B, Hoffman R, Shokat KM. Synthesis and
536 evaluation of indazole based analog sensitive Akt inhibitors. Mol Biosyst. 2010;6(8):1389-402.

537 24. Okuzumi T, Fiedler D, Zhang C, Gray DC, Aizenstein B, Hoffman R, et al. Inhibitor hijacking of
538 Akt activation. Nat Chem Biol. 2009;5(7):484-93.

539 25. Schoenborn JR, Tan YX, Zhang C, Shokat KM, Weiss A. Feedback circuits monitor and adjust
540 basal Lck-dependent events in T cell receptor signaling. Sci Signal. 2011;4(190):ra59.

541 26. Tan YX, Manz BN, Freedman TS, Zhang C, Shokat KM, Weiss A. Inhibition of the kinase Csk in
542 thymocytes reveals a requirement for actin remodeling in the initiation of full TCR signaling. Nat
543 Immunol. 2014;15(2):186-94.

544 27. Chow LM, Veillette A. The Src and Csk families of tyrosine protein kinases in hemopoietic cells.
545 Semin Immunol. 1995;7(4):207-26.

546 28. Zhu JW, Doan K, Park J, Chau AH, Zhang H, Lowell CA, et al. Receptor-like tyrosine
547 phosphatases CD45 and CD148 have distinct functions in chemoattractant-mediated neutrophil
548 migration and response to S. aureus. Immunity. 2011;35(5):757-69.

549 29. Tang R, Langdon WY, Zhang J. Regulation of immune responses by E3 ubiquitin ligase Cbl-b.
550 Cell Immunol. 2018.

551 30. Naramura M, Jang IK, Kole H, Huang F, Haines D, Gu H. c-Cbl and Cbl-b regulate T cell
552 responsiveness by promoting ligand-induced TCR down-modulation. Nat Immunol. 2002;3(12):1192-9.

553 31. Purev E, Neff L, Horne WC, Baron R. c-Cbl and Cbl-b act redundantly to protect osteoclasts
554 from apoptosis and to displace HDAC6 from beta-tubulin, stabilizing microtubules and podosomes. Mol
555 Biol Cell. 2009;20(18):4021-30.

556 32. Ueno H, Sasaki K, Honda H, Nakamoto T, Yamagata T, Miyagawa K, et al. c-Cbl is tyrosine-
557 phosphorylated by interleukin-4 and enhances mitogenic and survival signals of interleukin-4 receptor
558 by linking with the phosphatidylinositol 3'-kinase pathway. Blood. 1998;91(1):46-53.

559 33. Hunter S, Burton EA, Wu SC, Anderson SM. Fyn associates with Cbl and phosphorylates
560 tyrosine 731 in Cbl, a binding site for phosphatidylinositol 3-kinase. J Biol Chem. 1999;274(4):2097-
561 106.

562 34. Yi TL, Bolen JB, Ihle JN. Hematopoietic cells express two forms of lyn kinase differing by 21
563 amino acids in the amino terminus. Mol Cell Biol. 1991;11(5):2391-8.

564 35. Stanley E, Ralph S, McEwen S, Boulet I, Holtzman DA, Lock P, et al. Alternatively spliced
565 murine lyn mRNAs encode distinct proteins. Mol Cell Biol. 1991;11(7):3399-406.

566 36. Huang TH, Huo L, Wang YN, Xia W, Wei Y, Chang SS, et al. Epidermal growth factor receptor
567 potentiates MCM7-mediated DNA replication through tyrosine phosphorylation of Lyn kinase in human
568 cancers. Cancer cell. 2013;23(6):796-810.

569 37. Radivojac P, Vacic V, Haynes C, Cocklin RR, Mohan A, Heyen JW, et al. Identification,
570 analysis, and prediction of protein ubiquitination sites. Proteins. 2010;78(2):365-80.

571 38. Blom N, Sicheritz-Ponten T, Gupta R, Gammeltoft S, Brunak S. Prediction of post-translational
572 glycosylation and phosphorylation of proteins from the amino acid sequence. Proteomics.
573 2004;4(6):1633-49.

574 39. Verhagen AM, Wallace ME, Goradia A, Jones SA, Croom HA, Metcalf D, et al. A kinase-dead
575 allele of Lyn attenuates autoimmune disease normally associated with Lyn deficiency. J Immunol.
576 2009;182(4):2020-9.

577 40. Yokoyama N, Miller WT. Identification of residues involved in v-Src substrate recognition by site-
578 directed mutagenesis. FEBS Lett. 1999;456(3):403-8.

579 41. Xu W, Doshi A, Lei M, Eck MJ, Harrison SC. Crystal structures of c-Src reveal features of its
580 autoinhibitory mechanism. Mol Cell. 1999;3(5):629-38.

581 42. Brown MT, Cooper JA. Regulation, substrates and functions of src. Biochim Biophys Acta.
582 1996;1287(2-3):121-49.

583 43. Straus DB, Weiss A. Genetic evidence for the involvement of the lck tyrosine kinase in signal
584 transduction through the T cell antigen receptor. Cell. 1992;70(4):585-93.

585 44. Burgess KE, Odysseos AD, Zalvan C, Druker BJ, Anderson P, Schlossman SF, et al.
586 Biochemical identification of a direct physical interaction between the CD4:p56lck and Ti(TcR)/CD3
587 complexes. Eur J Immunol. 1991;21(7):1663-8.

588 45. Samelson LE, Phillips AF, Luong ET, Klausner RD. Association of the fyn protein-tyrosine
589 kinase with the T-cell antigen receptor. Proc Natl Acad Sci U S A. 1990;87(11):4358-62.

590 46. Goldsmith MA, Weiss A. Isolation and characterization of a T-lymphocyte somatic mutant with
591 altered signal transduction by the antigen receptor. Proc Natl Acad Sci U S A. 1987;84(19):6879-83.

592 47. Han J, Zhang G, Welch EJ, Liang Y, Fu J, Vogel SM, et al. A critical role for Lyn kinase in
593 strengthening endothelial integrity and barrier function. Blood. 2013;122(25):4140-9.

594 48. Yamamoto N, Takeshita K, Shichijo M, Kokubo T, Sato M, Nakashima K, et al. The orally
595 available spleen tyrosine kinase inhibitor 2-[7-(3,4-dimethoxyphenyl)-imidazo[1,2-c]pyrimidin-5-
596 ylamino]nicotinamide dihydrochloride (BAY 61-3606) blocks antigen-induced airway inflammation in
597 rodents. The Journal of pharmacology and experimental therapeutics. 2003;306(3):1174-81.

598 49. Buckbinder L, Crawford DT, Qi H, Ke HZ, Olson LM, Long KR, et al. Proline-rich tyrosine kinase
599 2 regulates osteoprogenitor cells and bone formation, and offers an anabolic treatment approach for
600 osteoporosis. Proc Natl Acad Sci U S A. 2007;104(25):10619-24.

601 50. Hanke JH, Gardner JP, Dow RL, Changelian PS, Brissette WH, Weringer EJ, et al. Discovery of
602 a novel, potent, and Src family-selective tyrosine kinase inhibitor. Study of Lck- and FynT-dependent T
603 cell activation. J Biol Chem. 1996;271(2):695-701.

604 51. Heng TS, Painter MW, Immunological Genome Project C. The Immunological Genome Project:
605 networks of gene expression in immune cells. Nat Immunol. 2008;9(10):1091-4.

606 52. Dwyer DF, Barrett NA, Austen KF, Immunological Genome Project C. Expression profiling of
607 constitutive mast cells reveals a unique identity within the immune system. Nat Immunol.
608 2016;17(7):878-87.

609 53. Gustin SE, Thien CB, Langdon WY. Cbl-b is a negative regulator of inflammatory cytokines
610 produced by IgE-activated mast cells. J Immunol. 2006;177(9):5980-9.

611 54. Shelby SA, Veatch SL, Holowka DA, Baird BA. Functional nanoscale coupling of Lyn kinase
612 with IgE-FcepsilonRI is restricted by the actin cytoskeleton in early antigen-stimulated signaling. Mol
613 Biol Cell. 2016;27(22):3645-58.

614 55. Kalesnikoff J, Galli SJ. Antiinflammatory and immunosuppressive functions of mast cells.
615 Methods Mol Biol. 2011;677:207-20.

616 56. Duan L, Reddi AL, Ghosh A, Dimri M, Band H. The Cbl family and other ubiquitin ligases:
617 destructive forces in control of antigen receptor signaling. Immunity. 2004;21(1):7-17.

618 57. Zhu LL, Luo TM, Xu X, Guo YH, Zhao XQ, Wang TT, et al. E3 ubiquitin ligase Cbl-b negatively
619 regulates C-type lectin receptor-mediated antifungal innate immunity. J Exp Med. 2016;213(8):1555-70.

620 58. Thien CB, Langdon WY. c-Cbl and Cbl-b ubiquitin ligases: substrate diversity and the negative
621 regulation of signalling responses. Biochem J. 2005;391(Pt 2):153-66.

622 59. Mohapatra B, Ahmad G, Nadeau S, Zutshi N, An W, Scheffe S, et al. Protein tyrosine kinase
623 regulation by ubiquitination: critical roles of Cbl-family ubiquitin ligases. Biochim Biophys Acta.
624 2013;1833(1):122-39.

625 60. Kyo S, Sada K, Qu X, Maeno K, Miah SMS, Kawauchi-Kamata K, et al. Negative regulation of
626 Lyn protein-tyrosine kinase by c-Cbl ubiquitin-protein ligase in FceRI-mediated mast cell activation.
627 Genes to Cells. 2003;8(10):825-36.

628 61. Shao Y, Yang C, Elly C, Liu YC. Differential regulation of the B cell receptor-mediated signaling
629 by the E3 ubiquitin ligase Cbl. J Biol Chem. 2004;279(42):43646-53.

630 62. Sanjay A, Houghton A, Neff L, DiDomenico E, Bardelay C, Antoine E, et al. Cbl associates with
631 Pyk2 and Src to regulate Src kinase activity, alpha(v)beta(3) integrin-mediated signaling, cell adhesion,
632 and osteoclast motility. J Cell Biol. 2001;152(1):181-95.

633 63. Sanjay A, Miyazaki T, Itzstein C, Purev E, Horne WC, Baron R. Identification and functional
634 characterization of an Src homology domain 3 domain-binding site on Cbl. FEBS J. 2006;273(23):5442-
635 56.

636 64. Palacios-Moreno J, Foltz L, Guo A, Stokes MP, Kuehn ED, George L, et al. Neuroblastoma
637 tyrosine kinase signaling networks involve FYN and LYN in endosomes and lipid rafts. PLoS Comput
638 Biol. 2015;11(4):e1004130.

639 65. Johnson TM, Williamson NA, Scholz G, Jaworowski A, Wettenhall RE, Dunn AR, et al.
640 Modulation of the catalytic activity of the Src family tyrosine kinase Hck by autophosphorylation at a
641 novel site in the unique domain. J Biol Chem. 2000;275(43):33353-64.

642 66. Teixeira J, Fuentes H, Bielskutė S, Gairi M, Żerko S, Koźmiński W, et al. The Two Isoforms of
643 Lyn Display Different Intramolecular Fuzzy Complexes with the SH3 Domain. Molecules. 2018;23(11).

644 67. Tornillo G, Knowlson C, Kendrick H, Cooke J, Mirza H, Aurrekoetxea-Rodriguez I, et al. Dual
645 Mechanisms of LYN Kinase Dysregulation Drive Aggressive Behavior in Breast Cancer Cells. Cell Rep.
646 2018;25(13):3674-92 e10.

647 68. Wynn TA, Chawla A, Pollard JW. Macrophage biology in development, homeostasis and
648 disease. Nature. 2013;496(7446):445-55.

649 69. Galli SJ, Borregaard N, Wynn TA. Phenotypic and functional plasticity of cells of innate
650 immunity: macrophages, mast cells and neutrophils. Nat Immunol. 2011;12(11):1035-44.

651 70. Bosurgi L, Cao YG, Cabeza-Cabrerizo M, Tucci A, Hughes LD, Kong Y, et al. Macrophage
652 function in tissue repair and remodeling requires IL-4 or IL-13 with apoptotic cells. Science.
653 2017;356(6342):1072-6.

654 71. Gentek R, Ghigo C, Hoeffel G, Bulle MJ, Msallam R, Gautier G, et al. Hemogenic Endothelial
655 Fate Mapping Reveals Dual Developmental Origin of Mast Cells. Immunity. 2018;48(6):1160-71 e5.

656 72. Rafiq K, Kolpakov MA, Seqqat R, Guo J, Guo X, Qi Z, et al. c-Cbl inhibition improves cardiac
657 function and survival in response to myocardial ischemia. Circulation. 2014;129(20):2031-43.

658 73. Weiss A, Stobo JD. Requirement for the coexpression of T3 and the T cell antigen receptor on a
659 malignant human T cell line. J Exp Med. 1984;160(5):1284-99.

660 74. Phee H, Abraham RT, Weiss A. Dynamic recruitment of PAK1 to the immunological synapse is
661 mediated by PIX independently of SLP-76 and Vav1. Nat Immunol. 2005;6(6):608-17.

662 75. Myers MD, Sosinowski T, Dragone LL, White C, Band H, Gu H, et al. Src-like adaptor protein
663 regulates TCR expression on thymocytes by linking the ubiquitin ligase c-Cbl to the TCR complex. Nat
664 Immunol. 2006;7(1):57-66.

665 76. Zhu JW, Brdicka T, Katsumoto TR, Lin J, Weiss A. Structurally distinct phosphatases CD45 and
666 CD148 both regulate B cell and macrophage immunoreceptor signaling. Immunity. 2008;28(2):183-96.

77. Takeshita S, Kaji K, Kudo A. Identification and characterization of the new osteoclast progenitor with macrophage phenotypes being able to differentiate into mature osteoclasts. Journal of bone and mineral research : the official journal of the American Society for Bone and Mineral Research. 2000;15(8):1477-88.

## Acknowledgements

We thank Arthur Weiss, Kevan Shokat, Yoji Shimizu, Brandon Burbach, Erik Peterson, Juan Rivera, and Ryo Suzuki for reagents and discussion and Terri Kadlecek, Marianne Mollenauer, and Whitney Swanson for technical support. Many thanks also to Hai-Bin Ruan, John Connett, Marc Jenkins, Bryce Binstadt, Erik Peterson, Nicholas Levinson, Aditi Bapat, Frances Sjaastad, and Emily Ewan for valuable discussions and feedback.

## Funding

This work was supported by NIH grants R01AR073966 (TSF), R03AI130978 (TSF) and R01CA215052 (KLS) and the following University of Minnesota awards (all TSF): Masonic Cancer Center/American Cancer Society IRG-58-001-55; Grant-in-Aid of Research, Artistry, and Scholarship #92286; University of Minnesota Foundation Research and Equipment Award NF-0315-02; and Center for Autoimmune Diseases Research Pilot Grant 2017. Training support was provided by NIH award T32DA007097 (BFB).

## Author Contributions

Conceptualization, Methodology, and Data Curation: BFB, TSF

Investigation, Validation, and Visualization: BFB, MGN, TSF

Formal Analysis, Writing- Review and Editing: BFB, MGN, KLS, TSF

Writing- Original Draft: BFB, TSF

Funding Acquisition: BFB, KLS, TSF

690 Project Administration, Resources, Validation, and Software: TSF

691 Supervision: KLS, TSF

## 692 Competing Interests

693 The authors state that they have no competing interests.

## 694 Data and Materials Availability

695 Reagents and protocols will be provided upon request.

## 696 Figure Supplements

697 **Figure 1–figure supplement 1. Loss of positive signaling in c-Cbl-deficient cells prevents**
698 **assessment of LynA contributions to Erk phosphorylation.**

699 **Figure 3–figure supplement 1. LynA$^{Y32A}$ and LynB are expressed more highly in Jurkat cells than**
700 **wild-type LynA.**

## 701 Source Data

702 Figure 1–Source Data 1

703 Figure 3–Source Data 1

704 Figure 3–figure supplement 1-Source Data 1

705 Figure 4–Source Data 1

706 Figure 5–Source Data 1

707 Figure 6–Source Data 1